Journal of Micromechanics and Microengineering

PAPER

# Rapid characterization of the biomechanical properties of drug-treated cells in a microfluidic device

To cite this article: Xiaofei Zhang *et al* 2015 *J. Micromech. Microeng.* **25** 105004

View the article online for updates and enhancements.

Related content

- Electrodeformation for single cell mechanical characterization
Jian Chen, Mohamed Abdelgawad, Liming Yu et al.
- Microsystems for cellular force measurement: a review
Xiaoyu Rayne Zheng and Xin Zhang
- The effect of neighboring cells on the stiffness of cancerous and non-cancerous human mammary epithelial cells
Xinyi Guo, Keith Bonin, Karin Scarpinato et al.

Recent citations

- Application of level-set method in simulation of normal and cancer cells deformability within a microfluidic device
Arman Mirzaaghaian *et al*
- Microfluidic device for rapid investigation of the deformability of leukocytes in whole blood samples
Anas Mohd Noor *et al*
- Analysis of red blood cell deformability using parallel ladder electrodes in a microfluidic manipulation system
Wanting Li *et al*


IOP ebooks™

Bringing together innovative digital publishing with leading authors from the global scientific community.

Start exploring the collection–download the first chapter of every title for free.

This content was downloaded from IP address 202.125.195.7 on 07/05/2021 at 18:57

IOP Publishing Journal of Micromechanics and Microengineering
J. Micromech. Microeng. **25** (2015) 105004 (10pp) doi:10.1088/0960-1317/25/10/105004

# Rapid characterization of the biomechanical properties of drug-treated cells in a microfluidic device

**Xiaofei Zhang[1,2,4,6], Henry K Chu[3,6], Yang Zhang[1], Guohua Bai[1,2], Kaiqun Wang[5], Qiulin Tan[1,2] and Dong Sun[1,2,3]**

[1] Key Laboratory of Instrumentation Science & Dynamic Measurement, Ministry of Education, North University of China, Taiyuan, People's Republic of China
[2] Science and Technology on Electronic Test & Measurement Laboratory, North University of China, Taiyuan, People's Republic of China
[3] Department of Mechanical and Biomedical Engineering, City University of Hong Kong, Hong Kong, People's Republic of China
[4] Department of Mechanical Engineering, The Hong Kong Polytechnic University, Hong Kong, People's Republic of China
[5] Department of Biomedical Engineering, College of Mechanics, Taiyuan University of Technology, Taiyuan, People's Republic of China

E-mail: medsun@cityu.edu.hk

Received 15 May 2015, revised 4 July 2015
Accepted for publication 23 July 2015
Published 8 September 2015


**Abstract**

Cell mechanics is closely related to many cell functions. Recent studies have suggested that the deformability of cells can be an effective biomarker to indicate the onset and progression of diseases. In this paper, a microfluidic chip is designed for rapid characterization of the mechanics of drug-treated cells through stretching with dielectrophoresis (DEP) force. This chip was fabricated using PDMS and micro-electrodes were integrated and patterned on the ITO layer of the chip. Leukemia NB4 cells were considered and the effect of all-trans retinoic acid (ATRA) drug on NB4 cells were examined via the microfluidic chip. To induce a DEP force onto the cell, a relatively weak ac voltage was utilized to immobilize a cell at one side of the electrodes. The applied voltage was then increased to 3.5 $V_{pp}$ and the cell started to be stretched along the applied electric field lines. The elongation of the cell was observed using an optical microscope and the results showed that both types of cells were deformed by the induced DEP force. The strain of the NB4 cell without the drug treatment was recorded to be about 0.08 (time $t = 180$ s) and the drug-treated NB4 cell was about 0.21 (time $t = 180$ s), indicating a decrease in the stiffness after drug treatment. The elastic modulus of the cell was also evaluated and the modulus changed from 140 Pa to 41 Pa after drug treatment. This microfluidic chip can provide a simple and rapid platform for measuring the change in the biomechanical properties of cells and can potentially be used as the tool to determine the biomechanical effects of different drug treatments for drug discovery and development applications.

Keywords: dielectrophoresis, stretching, stiffness, leukemia cell, drug treatment

(Some figures may appear in colour only in the online journal)

## 1. Introduction

The biomechanical properties of a cell play an important role in understanding many cellular processes, such as cell division, cell migration and apoptosis [1–3]. Within a cell, the cytoskeleton, which is a microscopic network of protein filaments and microtubules in the cytoplasm, is responsible for maintaining the shape and structural integrity of the cell. In recent years, several studies have indicated that cancer and

[6] These authors contributed equally to this work.

 © 2015 IOP Publishing Ltd Printed in the UK

other human diseases can cause disruption to the cytoskeleton organization, leading to a change in the biomechanical properties of the cells as compared to the original healthy cells [4, 5]. For instance, fibroblast cells that were transformed with monooncogenic *N-RAS*, viral and cells of tumor origin, respectively, were found to be 40–80% softer than the non-transformed cells [6]. Metastatic cancer cells obtained from patients were also found to be softer than the benign counterparts [7]. Cancer cells with high migratory and invasive potential could experience a decrease in the stiffness for up to five times [8]. Similarly, the modulus and viscosity of the transformed human chondrosarcoma cells were found to be lower than the normal ones [9]. Hence, the stiffness of a cell could potentially be used as the biomarker for determining the onset and progression of different diseases.

Nowadays, there are several techniques that can be used to evaluate the biomechanical properties of a cell, which include micropipette aspiration [10–12], mechanical probing [13–16], and structure-induced deformation [17, 18]. The micropipette aspiration technique applies a suction pressure to deform and pull the cell into the pipette. By monitoring the deformation of the cell in the pipette, different parameters can be measured to estimate the elastic modulus of the cell. This technique is capable of producing a large force ranging from 10 pN to 10 $\mu$N on the cell, but the precision of this contact-based approach is highly dependent on the experience of the operator as well as the experimental setup to minimize medium evaporation [11]. The mechanical probing technique, for example, atomic force microscopy (AFM), is another contact-based approach that uses a tool to characterize the cell directly. This technique can provide precise quantification of the applied force on the cell. However, limitations from this technique include low throughput [19] and the requirement of specific micro-wells for non-adherent cell trapping [20]. In addition to direct cell probing, cell deformation can also be induced by squeezing cells through narrow channels or other structures. With this structure-induced technique, the parameters such as the cell volume and the adhesion between the cell membrane and the channel walls are coupled to the deformability of a cell. Hence, variations between cell types, especially for sticker cells, may lead to errors in the measurements [21]. Also, the computational models and correlations between the passage time evaluated through the chip and the elastic modulus of the cell are still relatively preliminary [18].

Non-contact techniques such as optical stretcher [22, 23], magnetic twisting cytometry [24–26] and dielectrophoresis [19, 27–32] have also been proposed for the evaluation and analysis of cell properties. These techniques possess the advantages of minimizing the invasiveness and potential bacterial contamination on the cells. The optical stretcher technique employs two non-focused laser beams to trap a target cell and cell deformation is achieved by the induced surface forces from the beams. Nevertheless, one key limitation of the optical approach is that the force generated is relatively weak, which limits the types of cells to be examined [17]. The magnetic twisting cytometry technique utilizes magnetic forces to twist the cells through the magnetic beads attached to the surface of the cells. For this technique, the beads are arbitrary attached to the cells and hence, deviation in the bead positions between different cells may cause discrepancy in the measurements [24]. Among these techniques, dielectrophoresis has been regarded as one of the most efficient ways for non-contact cell manipulation and characterization. This method uses non-uniform electric fields through an electrode pair to polarize and deform cells, and the hardware setup is relatively simple. High throughput can be achieved by employing an array of micro-wells or a longer electrode pair. With advances in microfabrication technology, micro-chips with different integrated micro-electrode designs have been studied for characterizing the mechanical properties of various cells via dielectrophoresis stretching. For instance, MacQueen *et al* [27] employed a planar micro-electrode array to characterize the mechanical properties of mammalian cells. Different cells were examined and their elastic moduli were computed through the modeling equations proposed. Guido *et al* [19] examined the deformation responses for cancerous and noncancerous cells. The results suggested that electrode-formation can be used to unambiguously distinguish these two cell types due to their differences in the microtubule structures. Although the DEP technique has been reported for more than a decade, the number of studies is still limited [28]. Majority of the DEP research mainly focuses on the evaluation of the cell deformation [19, 30] and biophysical properties of a cell such as the membrane capacitance and the cytoplasm conductivity [29, 31–33]. Little work has been conducted on the characterization of the elastic moduli of diseased cells via DEP-based deformability tests. In light of this, this work proposes the development of a DEP-based microfluidic device for rapid characterization of the biomechanical properties of cells.

To quantify the biomechanical properties of a cell from the experimental data, different modeling equations have been developed to correlate the deformation response of a cell with its elastic modulus. For intentation-based experiments, the Hertz model is commonly used to evaluate the modulus of a cell, where the cell membrane is approximated as a smooth hemispherical boundary [12]. In contrast, the Brush model assumes the cell is surrounded with a brush of molecular components and protrusions [34]. For the magnetic twisting cytometry technique, the modulus equation can be expressed as a function that consists of parameters such as the applied force from the mechanism, the bead surface and the resulting bead translation or rotation [35]. To account for the time-dependent deformation behavior of cells, the standard linear solid (SLS) model and the power-law fluid model can be employed to derive the modulus of the cell from the data [36]. Table 1 summarizes the elastic modulus evaluated by different research groups. A more comprehensive summary on the modulus from different cell types can be referenced to the work by Rodriguez *et al* in [36] and Garard *et al* in [37].

In this paper, a microfluidic chip is designed for rapid characterization of the cells treated with anti-cancer drug. Based on the working principle of dielectrophoresis (DEP) stretching [19, 27–32], this microfluidic chip utilizes the cell biomechanics as the biomarker to examine the effectiveness of the drug delivered onto the cells. Comparing to other conventional characterization techniques such as AFM and optical indentation, this low-cost DEP-based microfluidic

**Table 1.** Biomechanical properties of different cell types.

| Cell type | Method | Model | Value |
|---|---|---|---|
| Chondrocytes (cartilage) | Micropipette | Viscoelastic solid | 650 Pa [11] |
| HL60 (leukemia) | AFM | Hertz | 855 ± 670 Pa [12] |
| Jurkat (leukemia) | AFM | Hertz | 48 ± 35 Pa [12] |
| K562 (leukemia) | AFM | Hertz | 200 Pa [21] |
| K562 + dexamethasone | AFM | Hertz | 4300 Pa [21] |
| K162 (leukemia) | Optical indentation | Hertz | 162.8 ± 19.2 Pa [38] |
| K162 + ATRA | Optical indentation | Hertz | 145.6 ± 25.4 Pa [38] |
| 3T3 (fibroblasts) | Optical stretcher | Actin cortex | 220 Pa [39] |
| NB4 (leukemia) | Optical stretcher | Creep compliance | 0.4 $Pa^{-1}$ [40] |
| NB4 + ATRA | Optical stretcher | Creep compliance | 0.6 $Pa^{-1}$ [40] |
| Macrophage (lung) | Magnetic twisting cytometry | Bead displacement | 1200 Pa [26] |
| SiHa (epithelial) | Dielectrophoresis | Finite element | 601 ± 183 Pa [28] |
| U937 (promonocytes) | Dielectrophoresis | Standard linear solid | 99 ± 44 Pa [27] |

chip does not require complex, bulky and expensive equipment to conduct the tests. Multiple cells can be immobilized onto a parallel micro-electrode design and stretched simultaneously. The microfluidic chip can also provide a controlled environment for cell assay and further characterization. In this work, human acute promyelocytic leukemia NB4 cells were chosen as the cancer cell type for the experiments. The cells were treated with all-trans retinoic acid (ATRA), a non-chemotherapy drug used to cure acute promyelocytic leukemia [41], and the change in the cell stiffness was characterized. By analyzing the degrees of cell elongation from the captured images, the elastic moduli were evaluated and compared with the results from other groups. This microfluidic chip thus provides a platform to evaluate the effectiveness of drug treatments for diseased cells.

## 2. Materials and methods

### *2.1. Cells and media*

Human acute promyelocytic leukemia NB4 cells were cultured in RPMI 1640 medium (Sigma, St Louis, MO), supplemented with 10% fetal bovine serum (Atlanta Biologicals, GA). ATRA was purchased from Sigma-Aldrich Co. (St. Louis, MO). To prepare the ATRA stock solution, ATRA was first dissolved in absolute ethanol to obtain a concentration of 100 $\mu$mol $L^{-1}$ and the solution was diluted with RPMI medium to a final concentration of 1 $\mu$mol $L^{-1}$. Before the experiment, cells incubated at 37°C in an atmosphere of 5% $CO_2$ were transferred to two culture dishes. For drug treatment, the medium in one of the dishes was changed to the ATRA containing culture medium and incubated for 3 d. After 3 d, cells from the two dishes were centrifuged and the cell pellets were resuspended to an isotonic buffer medium for the stretching experiments. This medium contains 8.5% sucrose, 0.3% dextrose and 20 mg $L^{-1}$ $CaCl_2$, which allows positive dielectrophoresis force to be induced on the cells [42], [43]. The electrical conductivity and the relative permittivity of the medium are approximately 10 mS $m^{-1}$ and 78, respectively. To ensure the cells in a healthy state, the experiments were performed and completed in one hour.

### *2.2. Cell deformation and elastic modulus estimation through dielectrophoresis*

Dielectrophoresis (DEP) is the movement of dielectric particles in a non-uniform electric field [44]. The strength of the DEP force acting on a lossless dielectric sphere with a permittivity $\varepsilon_p$ and radius $r$, is [45]:

$$F_{DEP} = 2\pi\varepsilon_m r^3 \mathrm{Re}[f_{CM}]\,\nabla E_{rms}^2 \quad (1)$$

where $f_{CM}$ is the Clausius–Mossoti factor, $\varepsilon_m$ is the permittivity of the suspending medium, Re[$f_{CM}$] is the real part of the $f_{CM}$, and $E_{rms}$ is the root-mean-squared strength of the supplied electric field. The Clausius–Mossoti factor, $f_{CM}$, can be represented as follows:

$$f_{CM} = \frac{\varepsilon_p^* - \varepsilon_m^*}{\varepsilon_p^* + 2\varepsilon_m^*} \quad (2)$$

where $\varepsilon^*$ is the complex permittivity, which is calculated by $\varepsilon^* = \varepsilon - j\sigma/\omega$. $\sigma$ is the conductivity, and $\omega$ is the frequency of electric field. Subscripts p and m denote the particle and the medium, respectively. When the particle is more polarizable than the medium, Re [$f_{CM}$] > 0 and the induced force pushes the particle towards the higher density region of electric field (p-DEP response). In contrast, when the particle is less polarizable than the medium, Re [$f_{CM}$] < 0 and the induced force repels the particle towards the lower density region of electric field (n-DEP response).

To induce a DEP force for cell deformation, two parallel micro-electrodes are used to trap multiple cells and generate the required non-uniform electric fields. At first, a low amplitude ac voltage is supplied to the micro-electrodes and the cells are brought into contact with one of the micro-electrodes by p-DEP. Since the voltage input is relatively low, cell deformations are not observable at this stage. In the subsequent step, the amplitude of the ac voltage is increased and higher electric field strength is generated from the micro-electrodes. The cells begin to deform, changing their shapes from spherical to ellipsoidal, along the electric field direction.

The DEP force acting on the cell can be computed using equation (1). The amount of stress, $\sigma_{stress}$, applied on the cell can be calculated by dividing the force equation with the

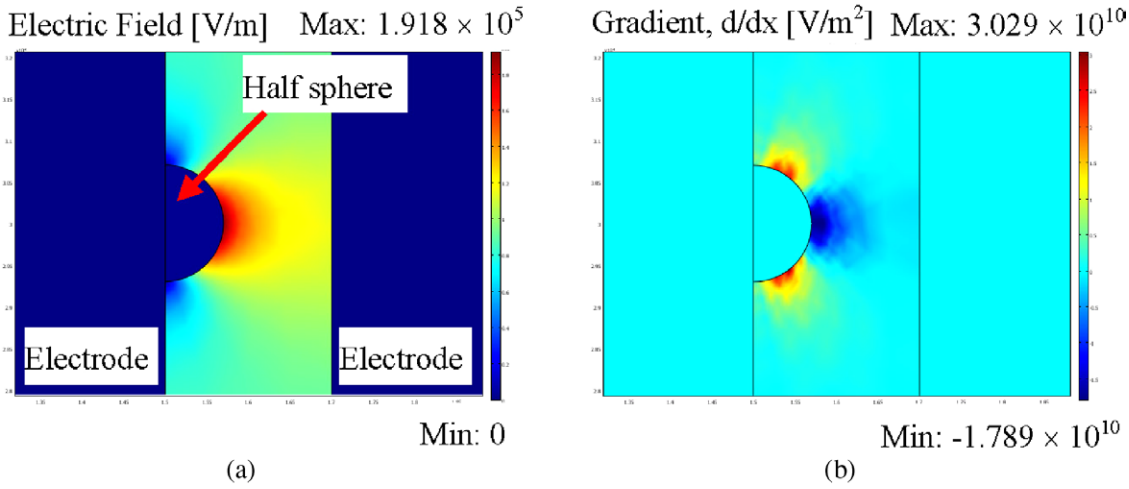


**Figure 1.** Simulation of the electric field distribution (top view): (a) in the presence of a half sphere; and (b) the resultant electric field gradient at one side of the sphere.

surface area of a half spherical cell and the stress equation can be further simplified as [27]:

$$\sigma_{\text{stress}} = n\text{Re}[f_{\text{CM}}]\,\varepsilon_{\text{m}}E_0^2 \tag{3}$$

$$n = \frac{E}{r\frac{\text{d}|E|}{\text{d}x}} \tag{4}$$

where $n$ is the geometric constant that can be obtained through COMSOL simulation. A 3.5 $V_{pp}$ voltage potential is set between the two 200 $\mu$m long electrodes with a 20 $\mu$m electrode gap as shown in figures 1(a) and (b). Free triangular mesh was used to discretize the region between the two electrodes. In presence of a half spherical cell with a radius of 7 $\mu$m, the electric field and the electric field gradient were simulated and the geometric constant, $n$, was calculated to be 1.5. The maximum electric field, $E_0$, which can be approximated using the 3.5 $V_{pp}$ voltage input and the 20 $\mu$m electrode gap, was evaluated to be 8.75 × $10^4$ V $m^{-1}$. The real part of the CM factor is closed to 1 at low frequency regime.

To determine the elastic moduli of the two cell types, the cells were modeled as a standard linear solid model. Under a normal stress, this model assumes the strain of the cell ($\gamma$) behaves like a spring ($k_1$) in parallel with a Maxwell material (a spring ($k_2$) in series with a damper ($\eta$)).The compliance function, $J(t)$, that describes the response of the material under the stress is [27]:

$$J(t) = \frac{\gamma}{\sigma} = \frac{1}{k_1}\left[1 - \left(\frac{k_2}{k_1 + k_2}\right)\text{e}^{-t/\tau_0}\right] \tag{5}$$

and the time constant, $\tau_0$, is:

$$\tau_0 = \eta\frac{(k_1 + k_2)}{k_1 k_2} \tag{6}$$

### *2.3. Fabrication of the microfluidic chip*

In order to provide an enclosed environment for the experiments, a microfluidic chip was designed and utilized as the platform to observe the cells under the microscope. PDMS was considered as the material for the chip because of its biocompatibility. A glass slide coated with electrically conductive, optically transparent indium tin oxide (ITO) was used to construct the parallel micro-electrodes. The schematic diagram and the image of the microfluidic chip are presented on figure 2.

The ITO micro-electrodes and the PDMS chip were fabricated using a photolithography process, as illustrated in figures 2(a)–(f). First, a positive photoresist (RZJ-304) was spin-coated onto the surface of the ITO glass (size: 25.4 × 76.2 mm), as shown in figure 2(a). Then, the coated ITO glass was exposed to UV light through a mask aligner and the parallel micro-electrode pattern on a chromium mask was transferred onto the photoresist. The patterned photoresist was developed using a developer solution and the unprotected ITO regions were etched away using an ITO etchant. After etching, the photoresist was removed and the ITO electrodes were formed as shown in figure 2(b). To fabricate the PDMS layer of the microfluidic chip, a 50 $\mu$m-thick photoresist (SU-8 2050) was spin-coated on a 2 in silicon wafer and used to define the microchannel of the chip (figure 2(c)). PDMS was cast into the fabricated SU-8 mold and cured in an oven at 65 °C for 4 h (figure 2(d)). The solidified PDMS was then peeled off from the mold and bonded onto the ITO glass with micro-electrodes using a plasma cleaner (figures 2(e) and (f)). The RF power was adjusted to 30 W and the vacuum pressure was set to 200 mTorr.

Figure 3 shows the enlarged view of the ITO micro-electrode design. The micro-electrode adopts a typical long electrode pair design with a fixed gap distance to generate the required electric fields for cell stretching. Similar micro-electrode designs have been previously reported in [19] and [30]. To minimize cell lysis or cell death, stretching of the cell was limited to be less than 1.5 times of its original size. For NB4 cells, the average diameter is approximately 14 $\mu$m and therefore a 20 $\mu$m electrode gap was adopted in the chip design for stretching. To induce positive DEP force onto the cell, the cell needs to be more polarizable than the surrounding medium and hence, the cells were suspended in the sucrose medium for the experiment.

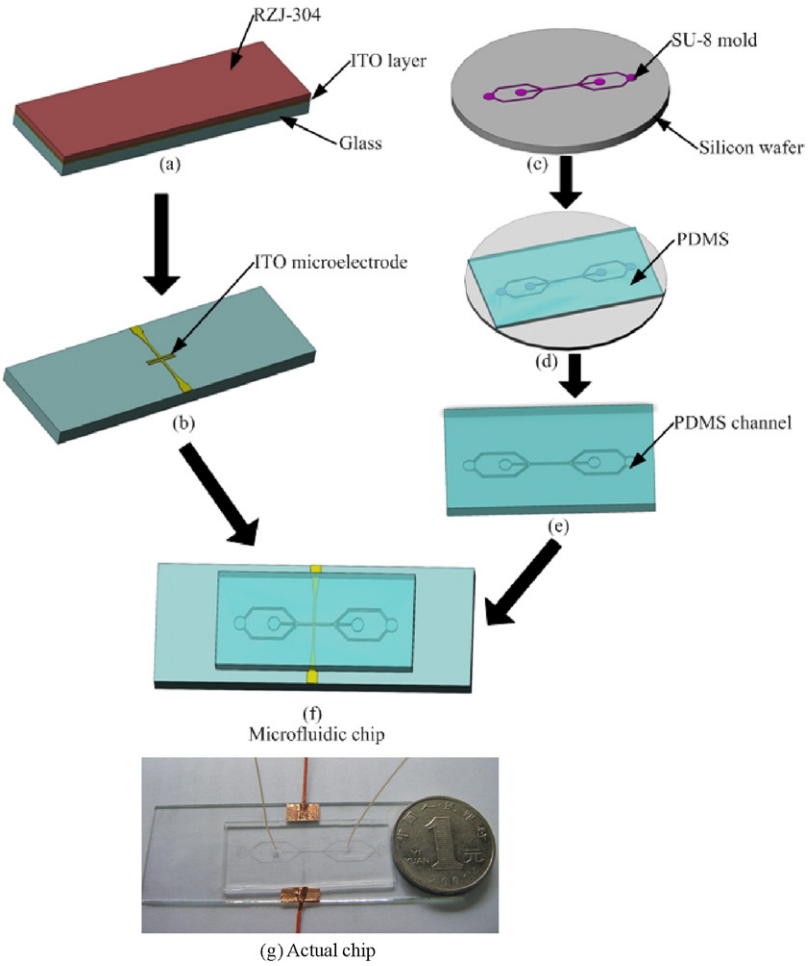


**Figure 2.** Fabrication procedure of ITO micro-electrode and PDMS microfluidic chip.

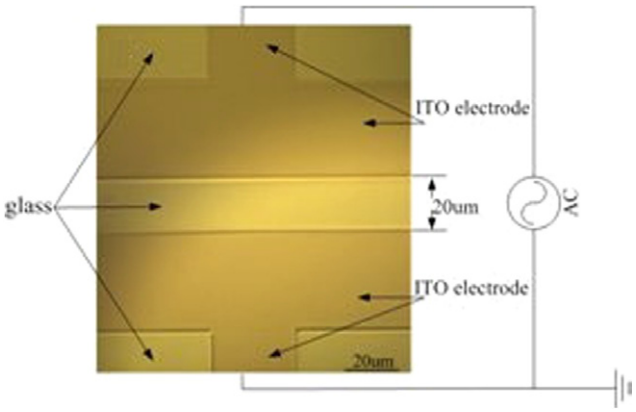


**Figure 3.** Image of the parallel ITO micro-electrodes under the microscope.

### *2.4. Cell trapping and stretching protocol*

The apparatus used to conduct the experiment is shown in figure 4. A LabSmith fluid flow control system was used to load the cell containing medium into the inlet of the microfluidic chip and to remove the cells from the chip after the experiments. A function generator (33120A, Agilent) was used to apply a sinusoidal signal to the ITO electrodes. The choice of the frequency is of utmost importance. When the frequency of the input voltage is low, the cell membrane behaves like an insulator and bears the most of the voltage drop, resulting cell lysis. If the frequency is too high, the cell acts like a homogeneous cytoplasm with the same permittivity as the surrounding medium, resulting smaller electrodynamic forces on the cells [28, 42]. In addition, the selected operating frequency must be in the frequency range at which the cells will experience positive DEP in the suspended medium. As reported in [46, 47], the cross-over frequency which leukemia cells such as HL60 and T cells changes from negative to positive DEP is at around 90 kHz and experiments employing positive DEP are typically operated at around 100 kHz to 1 MHz. Hence, a 500 kHz frequency was adopted in this work. To initiate the stretching experiment, a NB4 cell was attracted towards one of the electrodes by applying a 1.15 $V_{pp}$ voltage to the electrodes. At this voltage, no visible deformation on the cells was observed. After successful trapping of one cell, the voltage input was then increased to 3.5 $V_{pp}$. Since a higher DEP force was induced onto the cell, the imbalance forces between the two halves of the cell caused the cell to elongate along the electric field. The elongation of the cell was observed using an optical microscope with a CCD visual detection system (FO124SC, Foculus, Japan). The camera can provide a resolution of 200 nm to monitor the electrodeformation of the cells.

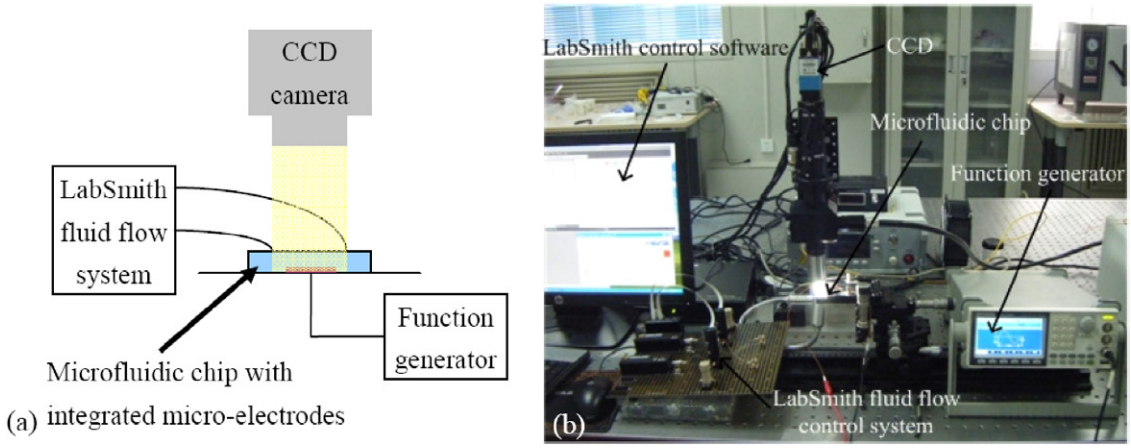


**Figure 4.** (a) Schematic diagram and (b) photograph of the experimental setup.

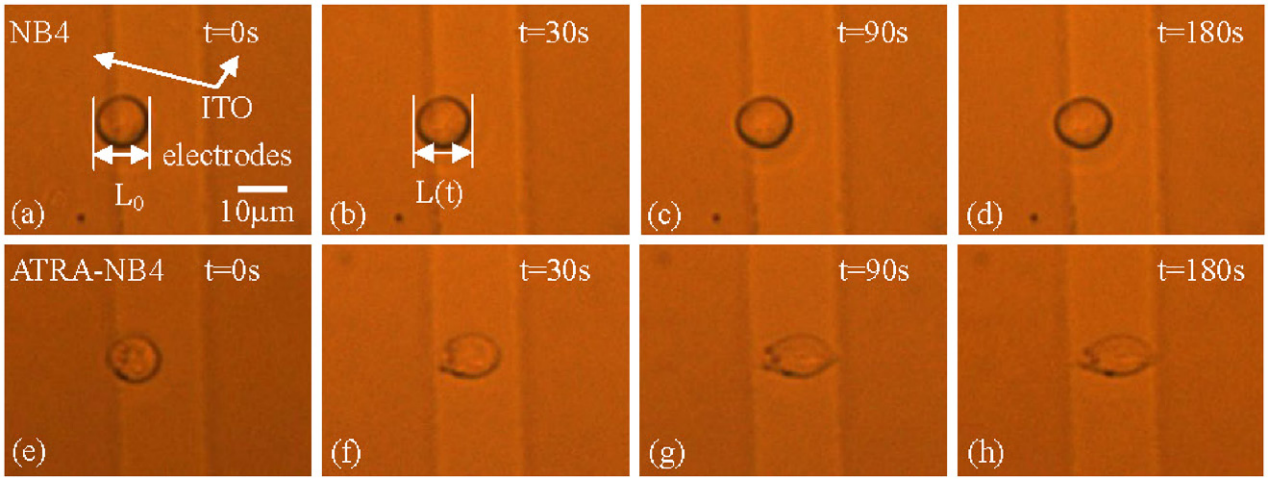


**Figure 5.** Images of a NB4 cell under the stretching experiment at different time intervals: (a) initial; (b) 30 s; (c) 90 s; (d) 180 s; Images of a NB4 cell treated with ATRA drug under the stretching experiment at different time intervals: (e) initial; (f) 30 s; (g) 90 s; (h) 180 s.

## 3. Results and discussion

The deformation of the cell under the DEP force was examined through the microfluidic chip. At every predefined interval, the CCD camera captured an image of the cell and the strain of the cell was evaluated using:

$$\gamma(t) = \frac{L(t) - L_0}{L_0} \tag{7}$$

where $L_0$ is the original diameter of the cell, $L(t)$ is the diameter of cell after stretching at time $t$. Image processing software, ImageJ, was used to measure the diameter in the captured images. Figures 5(a)–(d) illustrate images of a NB4 cell and figures 5(e)–(h) illustrate images of a drug-treated NB4 cell at different time intervals. In order to account for the slight variation on the biophysical properties between the cells, more than 40 cells were examined for each type ($N$ = 42 for NB4 and $N$ = 58 drug-treated NB4). The strain of the cells from each trial after 3 min was computed and summarized in figure 6. The data were grouped into strain intervals of 0.03, which is approximately equal to an elongation of 0.5 $\mu$m for a 14 $\mu$m NB4 cell. The results show that for NB4 cells, majority of the cells have an average strain value of around 0.06 to 0.09 and the maximum strain value is only 0.22. In contrast, for ATRA-NB4 cells, a large number of cells have an average strain value of 0.18 or above and some of these cells (in >0.30 category) could even be stretched until they reached the opposing electrode in less than 3 min. According to the results, a strain value of 0.2 can be considered as the threshold value for this microfluidic chip to distinguish between NB4 and ATRA-treated NB4 cells. The results also indicated NB4 cells treated with ATRA for 3 d were softer than the untreated ones and this finding is in agreement with other studies as reported in [38] and [40]. In theory, the effect of ATRA in leukemia cells is to induce differentiation of immature promyeloblasts into mature granulocytes, leading a decrease in the stiffness due to remodeling of the actin filament network [20, 40, 41]. From the results, the strain of the two cell types examined have a relatively scattered and board distribution. The possible reasons could be due to the influence of the physiological conditions such as the pH value and the temperature on the cell properties and the different life cycle phase of the cells, where cells are stiffer when they enter the later phases in their life cycle [38].

Based on the obtained results, NB4 cells treated with ATRA drug are more deformable and many of them could be

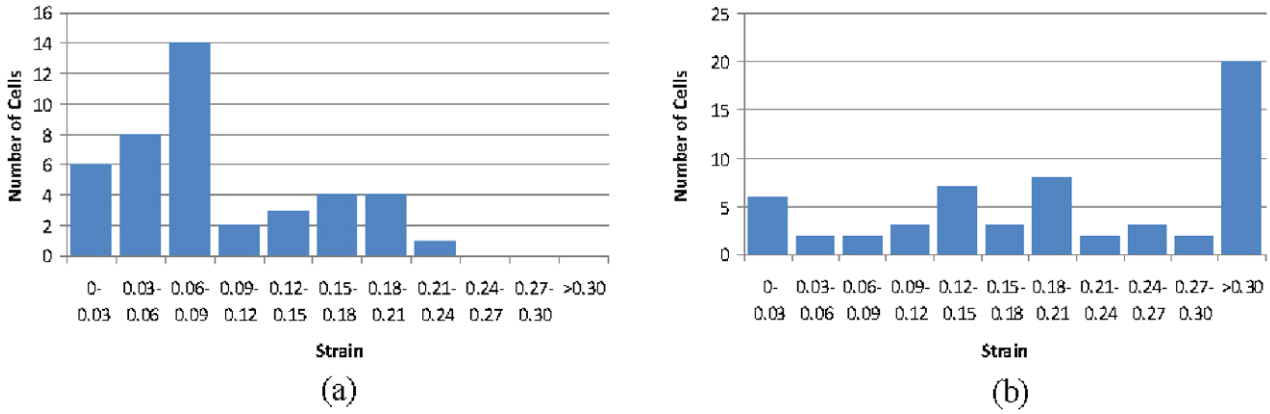


**Figure 6.** The number of cells at different strain values: (a) NB4 cells; (b) ATRA-NB4 cells.

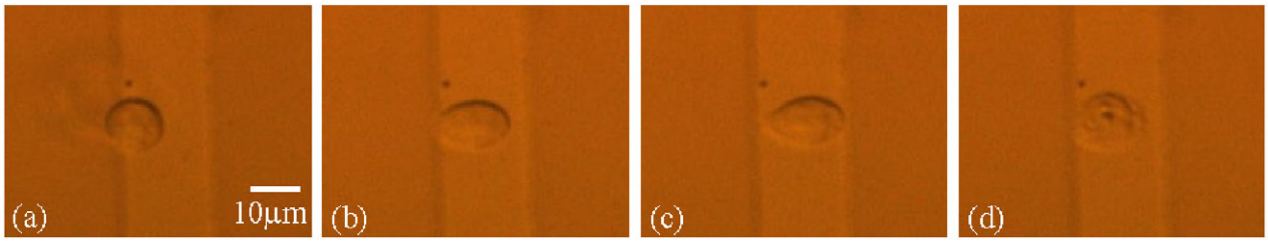


**Figure 7.** ATRA-NB4 cell (a) at its original size before DEP stretching; (b) during stretching; (c) fully stretched to the opposing electrode; (d) after cell lysis.

stretched from one electrode to the opposing electrode, which can be visually observed from the captured images as shown in figure 5 previously. Since the gap distance between the two electrodes was set to 20 $\mu$m, the cell was deformed by approximately 150%. Such level of deformation could cause damages to the cell and the cell would be unable to restore back to its original size even if the applied voltage was turned off. In addition, the 150% elongated cell could form a conductive path between the electrodes for electrical current flow, which would lead to rapid cell lysis. This phenomenon was more apparent when a higher DEP voltage (6.5 $V_{pp}$) was used, as shown in figure 7.

During the experiments, the cells were transferred and kept in a low conductivity isotonic buffer medium as discussed in section 2.1. In order to evaluate the effect of the medium on the cell viability, the cell containing medium was examined with Trypan Blue. The results show that even if the cells were kept in the isotonic medium for 1 h, at least 80% of the cells remain viable, as illustrated in figure 8.

The collected experimental data were also used to compute the biomechanical properties of the two cell types. Five sets of data from the NB4 cells with 0.06 to 0.09 strain values and five sets of data from the ATRA-NB4 cells with 0.18 to 0.24 strain values were selected and used to plot the average strain values over times, as shown in figure 9. After exposing the cells to the electric fields for 180 s, the average strain rate for NB4 cells was estimated to be 0.08 while the average strain rate for ATRA-NB4 cells was 0.21.

The strain data obtained from the experiment and the stress acting on the cell were calculated and substituted into equation (5) to determine the three unknown parameters in the visco-elastic model. The least square curve-fitting (lsqcurvefit)

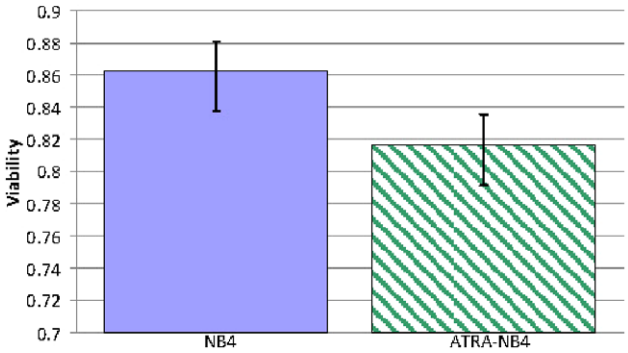


**Figure 8.** Cell viability for NB4 cells and ATRA-NB4 cells in an isotonic medium.

function in Matlab was used to estimate the parameters that can minimize the sum of squared residuals between the compliance function (equation (5)) and the best-fit model function. Since the compliance function was at the range of $1 \times 10^{-3}$, the termination tolerance, or the exit condition of the fitting process, was increased to $1 \times 10^{-11}$ and the results were listed in table 2. The average elastic modulus of untreated NB4 cell was 140.11 Pa while the average elastic modulus of drug-treated cell was 41.53 Pa. Similar observations in the decrease in moduli for drug-treated cells are reported in K562 (162.8 Pa) and ATRA-K562 (145.6 Pa) leukemia cells as determined using the optical indentation method [38]. Although five sets of data were included in this work to account for the slight variation between cells, the discrepancy in the moduli as evaluated through the fitting process was still relatively large. The reason could be mainly due to the difficulty in measuring the small deformation of the cells accurately from the captured images.

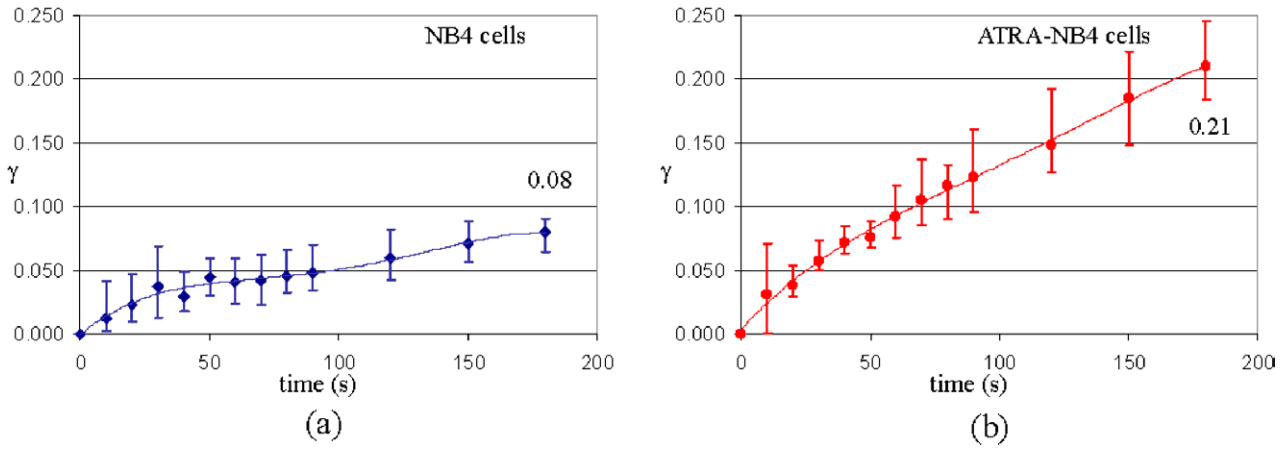


**Figure 9.** Strain versus time for: (a) NB4 cells; (b) ATRA-NB4 cells.

**Table 2.** Biomechanical properties of NB4 and ATRA-NB4 cells.

| | $k_1$ (Pa) | $k_2$ (Pa) | $\eta$ (Pa * s) |
|---|---|---|---|
| NB4 Cells | 140.11 ± 82.04 | 4224.27 ± 3896.23 | 27267.37 ± 15494.22 |
| ATRA-NB4 cells | 41.53 ± 27.82 | 2332.34 ± 2098.93 | 11325.53 ± 3072.75 |

In this work, the elastic modulus of leukemia NB4 cells was estimated through the DEP stretching technique and the accuracy of this technique is mainly dependent on two parameters: the applied DEP force and the employed model. As indicated in equation (1), the DEP force acting on the cell is not a constant, uniform force and it varies with the electric field over time. Also, the strength of the DEP force is affected by the cell position as the cell is stretched along the electric field. However, in the computation, a uniaxial force is assumed to be applied on the cell during the entire cell deformation experiment. The complexity of the DEP working principle also makes this technique difficult to perform force calibration with other specimens as the DEP force is correlated to unique properties such as the dielectric properties of the cells, the cell size and the medium. In this work, the standard linear solid model is selected to estimate the modulus of the cell and the cell is assumed to be a viscoelastic solid body under the DEP stretching force. Schmid *et al* [48] has reported that this model can accurately estimate the biomechanical properties of leukocytes. Nevertheless, other reports have also indicated that the liquid droplet model can better characterize the plasma membrane and the cytoplasmic viscosity of leukocytes under persistent tension [12, 49]. Although several models have been proposed and examined, these models are mostly derived based on the assumptions or experimental conditions for a particular cell deformation technique, which may not be applicable to other cell deformation techniques. Hence, further investigation should be conducted to examine the elastic modulus for the same cell type with different techniques in order to obtain a more comprehensive data for comparison.

## 4. Conclusions

This paper presents the design and development of a microfluidic chip for rapid characterization of drug-treated cells via dielectrophoresis stretching. Parallel ITO micro-electrodes integrated in the chip were used to generate electric fields in the environment, inducing a DEP force on the cell for stretching. Two types of cells, NB4 cells and NB4 cells treated with ATRA drug, were considered and the effect of the drug on the biomechanical properties of the cells were examined. To conduct the experiments, a relatively low ac voltage was first applied to the electrodes to attract a cell to one side of the electrodes via p-DEP force. The voltage input was then increased and the change in the cell size and shape was observed using optical microscope. Experimental results show that ATRA treated NB4 cells are softer than untreated ones. The simple microfluidic chip not only provides an efficient and low-cost tool to evaluate the biomechanical properties of leukemia cells based on electrodeformation, but also suggests a new method to determine the effects of various drugs on the cells, which can shorten the drug development period.

## Acknowledgments

This work was supported by ‘hundred talents program of Shanxi’, and also in part by a grant from the Research Grant Council of the Hong Kong Administrative Region, China (ref no. CityU 121513). The authors thank the staff of Department of Mechanical and Biomedical Engineering, City University of Hong Kong, China, in particular Shuxun Chen, for their support to this work.

## References

[1] Nagayama M, Haga H and Kawabata K 2001 Drastic change of local stiffness distribution correlating to cell migration in living fibroblasts *Cell Motil. Cytoskeleton* **50** 173–9
[2] Starodubtseva M N 2011 Mechanical properties of cells and ageing *Ageing Res. Rev.* **10** 16–25

[3] Bausch A R and Kroy K 2006 A bottom-up approach to cell mechanics *Nat. Phys.* **2** 231–8

[4] Suresh S, Spatz J, Mills J P, Micoulet A, Dao M, Lim C T, Beile M and Seufferlein T 2005 Connections between single-cell biomechanics and human disease states: gastrointestinal cancer and malaria *Acta Biomater.* **1** 15–30

[5] Lee G Y H and Lim C T 2007 Biomechanics approaches to studying human diseases *Trends Biotechnol.* **25** 111–8

[6] Efremov Y, Lomakina M E, Bagrov D V, Makhonovskiy P I, Alexandrova A Y, and Kirpichnikov M P 2014 Mechanical properties of fibroblasts depend on level of cancer transformation *Biochimica et Biophys. Acta (BBA)—Mol. Cell Res.* **1843** 1013–9

[7] Cross S E, Jin Y S, Rao J Y and Gimzewski J K 2007 Nanomechanical analysis of cells from cancer patients *Nat. Nanotechnol.* **2** 780–3

[8] Swaminathan V, Mythreye K, O'Brien E T, Berchuck A, Blobe G C and Superfine R 2011 Mechanical stiffness grades metastatic potential in patient tumor cells and in cancer cell lines *Cancer Res.* **71** 5075–80

[9] Darling E M, Zauscher S, Block J A and Guilak F 2007 A thin-layer model for viscoelastic, stress-relaxation testing of cells using atomic force microscopy: do cell properties reflect metastatic potential *Biophys. J.* **92** 1784–91

[10] Evans E A and Hochmuth R M 1976 Membrane viscoelasticity *Biophys. J.* **16** 1–11

[11] Hochmuth R M 2000 Micropipette aspiration of living cells *J. Biomech.* **33** 15–22

[12] Rosenbluth M J, Lam W A and Fletcher D A 2006 Force microscopy of nonadherent cells: a comparison of leukemia cell deformability *Biophys. J.* **90** 2994–3003

[13] Warnat S, King H, Forbrigger C and Hubbard T 2015 PolyMUMPs MEMS device to measure mechanical stiffness of single cells in aqueous media *J. Micromech. Microeng.* **25** 025011

[14] Xiao L, Tang M, Li Q and Zhou A 2013 Non-invasive detection of biomechanical and biochemical responses of human lung cells to short time chemotherapy exposure using AFM and confocal Raman spectroscopy *Anal. Methods* **5** 874–9

[15] Zhao Y, Zhou J, Dai W, Zheng Y and Wu H 2011 A convenient platform of tunable microlens arrays for the study of cellular responses to mechanical strains *J. Micromech. Microeng.* **21** 054017

[16] Wang Q, Zhang X and Zhao Y 2013 Micromechanical stimulator for localized cell loading: fabrication and strain analysis *J. Micromech. Microeng.* **23** 015002

[17] Hou H W, Li Q S, Lee G Y H, Kumar A P, Ong C N and Lim C T 2009 Deformability study of breast cancer cells using microfluidics *Biomed. Microdevices* **11** 557–64

[18] Guan G, Chen P C Y, Peng W K, Bhagat A A, Ong C J and Han J 2012 Real-time control of a microfluidic channel for size-independent deformability cytometry *J. Micromech. Microeng.* **22** 105037

[19] Guido I, Jaeger M S and Duschl C 2011 Dielectrophoretic stretching of cells allows for characterization of their mechanical properties *Eur. Biophys. J.* **40** 281–8

[20] Lam W A and Fletcher D A 2011 Cellular mechanics of acute leukemia and chemotherapy *Cellular and Biomolecular Mechanics and Mechanobiology, Studies in Mechanobiology, Tissue Engineering and Biomaterials* (Berlin Heidelberg: Springer) vol 4 pp 523–58

[21] Zhang Y, Nguyen J, Wei Y and Sun Y 2013 Recent advances in microfluidic techniques for single cell biophysical characterization *Lab Chip* **13** 2464–83

[22] Wang K, Cheng J, Cheng S H and Sun D 2013 Probing cell biophysical behavior based on actin cytoskeleton modeling and stretching manipulation with optical tweezers *Appl. Phys. Lett.* **103** 083706

[23] Tan Y, Kong C, Chen S, Cheng S H, Li R A and Sun D 2012 Probing the mechanobiological properties of human embryonic stem cells in cardiac differentiation by optical tweezers *J. Biomech.* **45** 123–8

[24] Mijailovich S M, Kojic M, Zivkovic M, Fabry B and Fredberg J J 2002 A finite element model of cell deformation during magnetic bead twisting *J. Appl. Physiol.* **93** 1429–36

[25] Tanase M, Biais N and Sheetz M 2007 Magnetic tweezers in cell biology *Methods Cell Biol.* **83** 473–93

[26] Patel N R *et al* 2012 Cell elasticity determines macrophage function *PLoS One* **7** e41024

[27] MacQueen L A, Buschmann M D and Wertheimer M R 2010 Mechanical properties of mammalian cells in suspension measured by electro-deformation *J. Micromech. Microeng.* **20** 065007

[28] Chen J, Abdelgawad M, Yu L, Shakiba N, Chien W, Lu Z, Geddie W R, Jewett M A S and Sun Y 2011 Electrodeformation for single cell mechanical characterization *J. Micromech. Microeng.* **21** 054012

[29] Chen N, Chen C, Chen M, Jang L and Wang M 2014 Single-cell trapping and impedance measurement utilizing dielectrophoresis in a parallel-plate microfluidic device *Sensors Actuators B: Chem.* **190** 570–7

[30] Doh I, Lee W C, Cho Y, Pisano A P and Kuypers F A 2012 Deformation measurement of individual cells in large populations using a single-cell microchamber array chip *Appl. Phys. Lett.* **100** 173702

[31] Cen E G, Dalton C, Li Y, Adamia S, Pilarski L M and Kaler K 2004 A combined dielectrophoresis, traveling wave dielectrophoresis and electrorotation microchip for the manipulation and characterization of human malignant cells *J. Microbiol. Methods* **58** 387–401

[32] Labeed F H, Coley H M and Hughes M P 2006 Differences in the biophysical properties of membrane and cytoplasm of apoptotic cells revealed using dielectrophoresis *Biochim. et Biophys. Acta* **1760** 922–9

[33] Chen J, Li J and Sun Y 2012 Microfluidic approaches for cancer cell detection, characterization, and separation *Lab Chip* **12** 1753–67

[34] Dokukin M E, Guz N V and Sokolov I 2013 Quantitative study of the elastic modulus of loosely attached cells in AFM indentation experiments *Biophys. J.* **104** 2123–31

[35] Kamgoue A, Ohayon J and Tracqui P 2007 Estimation of cell Young's modulus of adherent cells probed by optical and magnetic tweezers: influence of cell thickness and dead immersion *J. Biomech. Eng.* **129** 523–30

[36] Rodriguez M L, McGarry P J and Sniadecki N J 2013 Review on cell mechanics: experimental and modeling approaches *Appl. Mech. Rev.* **65** 060801

[37] Girard P P, Cavalcanti-Adam E A, Kemkemer R and Spatz J P 2007 Cellular chemomechanics at interfaces: sensing, integration and response *Soft Matter* **3** 307–26

[38] Zhou Z L, Tang B and Ngan A H W 2010 The biomechanics of drug-treated leukemia cells investigated using optical tweezers *Nano Life* **1** 1–4

[39] Ananthakrishnan R *et al* 2006 Quantifying the contribution of actin networks to the elastic strength of fibroblasts *J. Theor. Biol.* **242** 502–16

[40] Lautenschlager F, Paschke S, Schinkinger S, Bruel A, Beil M and Guck J 2009 The regulatory role of cell mechanics for migration of differentiating myeloid cells *Proc. Natl Acad. Sci. USA* **106** 15696–701

[41] Adamson P C 1996 All-trans-retinoic acid pharmacology and its impact on the treatment of acute promyelocytic leukemia *Oncologist* **1** 305–14

[42] Puttaswamy S V, Sivashankar S, Chen R J, Chin C K, Chang H Y and Liu C H 2010 Enhanced cell viability and cell adhesion using low conductivity medium for negative dielectrophoretic cell patterning *Biotechnol. J.* **5** 1005–15

[43] Chu H K, Huan Z, Mills J K, Yang J and Sun D 2015 Three-dimensional cell manipulation and patterning using dielectrophoresis via a multi-layer scaffold structure *Lab Chip* **15** 920–30

[44] Pohl H A 1951 The motion and precipitation of suspensoids in divergent electric fields *J. Appl. Phys.* **22** 869–71

[45] Jones T B 1995 *Electromechanics of Particles* (Cambridge: Cambridge University Press) chapter 2

[46] Menachery A and Pethig R 2005 Controlling cell destruction using dielectrophoretic forces *IEEE Proc. Nanobiotechnol.* **152** 145–9

[47] Chin S, Hughes M P, Coley H M and Labeed F H 2006 Rapid assessment of early biophysical changes in K562 cells during apoptosis determined using dielectrophoresis *Int. J. Nanomed.* **3** 333–7

[48] Schmid-Schonbein G W Sung K L, Tozeren H, Skalak R and Chien S 1981 Passive mechanical properties of human leukocytes *Biophys. J.* **36** 243–56

[49] Zheng Y, Wen J, Nguyen J, Cachia M A, Wang C and Sun Y 2014 Decreased deformability of lymphoctyes in chronic lymphocytic leukemia *Sci. Rep.* **5** 7613